DESIGN OF A MECHANICALLY CLOSED-LOOP TEST RIG FOR TESTING AVIATION INDUSTRY'S GEARBOXES

Shadan MOZAFARI[1], Mehdi REZAZADEH MOHAMADI[2], Somaye DOLATKHAH TAKLOO[3], Mohsen MARDANI[4]

[1]*Mechanical engineering department, Sharif University of Technology, Azadi St., Tehran, Iran*
[1, 2, 3, 4]*Sharif University of Technology branch of ACECR, Azadi St., Tehran, Iran*
E-mails: [1]shad.mzf@gmail.com; [2]rezazadeh.mrm@gmail.com; [3]somayeh.dolatkhah@gmail.com; [4]mardani@jdsharif.ac.ir (corresponding author)

Shadan MOZAFARI, *Msc, Mechanical Eng.*
Education: 2012–2014, Bachelor of Mechanical Engineering,
AmirKabir University of Technology; 2014–2016, Master of Mechanical Engineering,
Sharif University of Technology.
Research interests: power transmission systems, vibration, and machining.
Present position: 2015–2016, researcher, Sharif University Branch of ACECR.

Mehdi REZAZADEH, *Msc, Mechanical Eng.*
Education: 2004–2008, Bachelor of Mechanical Engineering,
Isfahan University of Technology;
2008–2011, Master's degree in Mechanical Engineering,
Iran University Science and Technology.
Research interests: transmission technology, automation, 3D printing, and metal forming.
Publications: author of 2 Articles, over 5 conference papers, and 3 technical industry reports.
Present Position: since 2016, Mechanical Engineer in the ACECR Group.

Somayeh DOLATKHAH TAKLOO, *Msc. Electrical Eng.*
Education: 2001–2006, Bachelor of Electronics Engineering; 2007–2010,
Master of Control Engineering, AmirKabir University of Technology (Tehran Polytechnic).
Research interests: nonlinear system control, aircraft. system control, and disturbance observing in aviation systems.
Publication: author of 5 conference papers and 2 articles.
Present position: 2014–2016, researcher in the ACECR (Academic Centre of Education, Culture and Research).

Mohsen MARDANI, *Assistant Professor*
Education: 2000–2005, Bachelor of Electrical Engineering; 2005–2013, Master and PhD degrees, AmirKabir University of Technology; since 2013, research assistant, Nanyang Technological University, Singapore.
Research interest: test systems.
Publications: author of 20 papers, 2 books, and 16 technical industry reports.
Present positions: since 2015, Vice president of Research and Technology, Sharif University Branch of ACECR.

Abstract. Due to the wide usage of rotary equipment and the necessity of their testing for maintenance and repair, test rigs have become necessary. The mechanical closed-loop test rig developed in Sharif University of Technology branch of ACECR (Academic Centre of Education, Culture and Research) is a test rig with low energy losses that is

suitable for testing high power gearboxes such as aerospace or wind turbine gearboxes. It can be loaded up to 489Hp at a maximum speed of 3000 rpm, and the test components can be tested in different testing conditions including a variety of torques and speeds. This paper describes the preliminary, conceptual, and detailed design, steps including frame work design, control system design, hydraulic system and torque generator design asn well as a dynamic and static analysis of the whole system. Also a simplified model of the system is presented and qualified, and some data of test rig's working conditions is presented. These data includes the temperature change of the gearboxes, their vibration in time, and also the variation of torque, hydraulic pressure, and motor speed. Furthermore, the relation between these parameters is investigated to determine the behaviour of the system. The validity of the system's dynamic modelling is also investigated and verified.

Keywords: closed-loop test rig, gearbox test, mechanical energy regeneration, mechanically closed-loop, aviation gearbox test, power regeneration test rig.

1. Introduction

The test rig presented in this paper, which uses the hydraulic jack and planetary gearboxes for applying locked torque to it, is a special kind of system suitable for testing orthogonal gearboxes. Torsion is applied to the ring of the planetary gear due to the displacement of pistons in hydraulic cylinders, so the torque is applied to the system during the rotation of components generated by this torsion. The rotational speed required for producing the considered power is supplied by an electric motor which is controlled by a drive. Torque and rotational speed can be adjusted according to a specific tests' plans, because each of these parameters may be controlled, and it is possible to develop precise testing conditions. Power is transferred by shafts and gearboxes, and the couplings and connections prevent the transmission of moments to the gearboxes. Due to the symmetric design of the whole system and the related calculations, it is possible to use the rig for testing multiple gearboxes. Also, it is possible to determine the accuracy of such tests by moving the tested gearbox in different gearbox places within the loop in a single testing. The energy is circulated in the closed loop and the motor is just responsible for developing the maximum energy needed during the first step of setting up the system and also for supplying the wasted energy along the loop during the rest of the process. This allows performing the tests by using less energy. The system is also investigated dynamically and is designed in a way that the frequencies and vibrational characteristics of the system and the gearboxes are completely distinct; therefore the fault detection of gearboxes using vibrational methods is also possible. Consequently, by using the present test rig, accurate fault detection and testing of gearboxes in their operational condition can be performed with precisely controlled torques and speeds. The results show that the conceptual design of this closed-loop gearbox test rig can meet the design requirements and safety criterion.

2. Previous research

In the presented setup for testing orthogonal gearboxes, the idea of energy circulation in a closed loop is used.

Many closed-loop test rigs have been made and different usages have been defined and studied. For example, the wear of transmission chain using a closed-loop rig (Hollingworth 1987), and also the efficiency of a helicopter transmission planetary reduction stage by a closed-loop test rig (Handschuh, Rohn 1989) have been studied. Also, a mechanical closed-loop test rig for testing different gears has been presented, using which various gears with different geometries and materials were analysed (Manoj *et al.* 2003). In 2004, the automotive gearbox's endurance was determined using mechanical closed-loop testing. It was also demonstrated that it's possible to apply endurance tests to automotive gearboxes for a long time by using lower cost and energy (Miláček 2004). In 2010, a closed-loop test rig for fatigue testing of aviation gearboxes using numerical modelling was designed (Markowski *et al.* 2010). A thermal model of a back-to-back closed-loop test rig was presented in 2012 (de Gevigney *et al.* 2012). Moreover, the development of test rigs for evaluating the performance of the gear has been studied in addition to the fabrication and discussion of a new gear test rig having the same capability (Arun *et al.* 2014). The development of a computational method for the analysis of torque and rotation fluctuations in each shaft line of a power recirculation gear test rig has been proposed (Maia *et al.* 2014). The torque loss in gears lubricated with wind turbine gearbox's oil (Fernandes *et al.* 2014) and losses due to friction in gears were analysed and the results were compared with those from testing with a closed-loop test rig (Fernandes *et al.* 2015a) and also the energy losses in planetary and parallel gearboxes using closed-loop test rig (Fernandes *et al.* 2015b) have been investigated. Furthermore, a test bench to test a gearbox at the end of the assembly line to check leakage, noise, gear shifting feeling and shift load in driving and dragging condition has been designed (Khodwe, Prabhune 2015). In 2016, the efficiency of a wind turbine gearbox using the same system has been investigated (Fernandes *et al.* 2016), while a double-helical gear–rotor journal-bearing system test rig was designed to carry out experimental investigations in the dynamic behaviour of a double-helical gear system supported by journal bearings,

including the dynamic transmission errors of gear pairs (Yin *et al.* 2016).

3. System concept

Ageneral configuration of the test rig is shown in Figure 1. There are two similar planetary gearboxes in the system. One operates as a speed increaser, and the
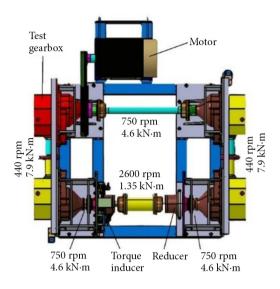

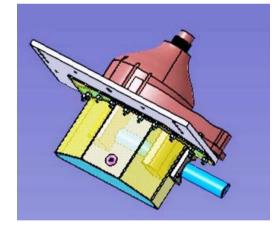Fig. 1. The test rig with nominal speeds and torques
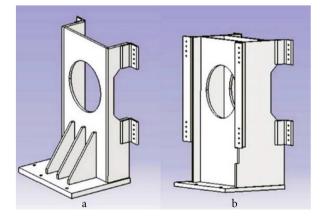

Fig. 2. Gearbox assembly

Fig. 3. Stands type 1 (a), and stand type 2 (b)

other – as a reducer. The first one is the gearbox used to apply lucked torque into the loop, and the latter one is used to decrease the output speed of the torque. Nominal speeds and torques are also showed in Figure 1.

Oil is used in the gearboxes as a coolant and lubricant. It is cooled off in the transducer and flows back to the gearboxes. The tests in this rig are performed and controlled by a control system. A truck's differential gearboxes are used in the loop as similar orthogonal gearboxes. Maximum input torque is 4.6 kN.m and the maximum speed is 750 rpm, and, since the truck's gearboxes can endure 14.5 kN.m torque and can operate at the speed of 2500 rpm, they can be used in this closed-loop test rig. For connecting the orthogonal gearboxes to the rig's chassis, a plate is used.

Gearboxes' oil cases are also made of a steel plate of 2 mm thickness. These cases are bolted to the gearboxes' holding plates using the connection bolts of the gearboxes and those plates. Gaskets are also used for sealing these connections.

The assembled gearbox with the holder plate, oil case, and output axes, is shown in Figure 2. Radial shaft seals are also used.

By investigating the efficiency of different gearboxes, the efficiency of the gearboxes used is assumed to be 98%. There are six gearboxes used in the loop, and by assuming the aforesaid efficiency, the amount of losses under the maximum operating power of 365 kW equals 35 kW, so the minimum power required for the motor is 35 kW. Therefore, due to the closest standard powers, a motor with a nominal power of 37 kW is chosen.

4. System design

4.1. Frame

As shown in Figure 1, the orthogonal gearboxes are placed in two different ways. In fact, there are two types of them. The first type are the ones which are placed independently, and then their input shafts are connected to each other. The second type are the ones which are connected to planetary gearboxes and should endure the weight of both the planetary and orthogonal gearboxes. As a result, two kinds of stands should be designed. These two types are shown in Figure 3.

Also, for reducing the displacement of the stands due to the applied forces, as shown in Figure 3, two reinforcement studs are used for connecting their top parts together.

For analysing the stresses and displacements in the structure, a finite element analysis is used in Abaqus. The results of these analyses are shown in Figures 4a and 4b. Torques and forces transferred to the gearboxes include the torque created in the system due to the motor's torque (as in Fig. 1) and the weight of components. Due to the orthogonal ordering of the gearboxes

in the system, these torques cause torsion in some parts of the system and a bending moment in the other parts. As seen in Figure 4a, the maximum value of stress is 50 Mpa. Considering the 370 Mpa as structural steel's yield strength, the safety factor is 7. Displacements are also shown in Figure 4b. The maximum displacement in this figure is 0.3 mm. This displacement should be compensated by use of couplings.

A simplified model is meshed in HyperWorks and analysed in Abaqus for finding the natural frequencies of the structure to check the resonance. The masses of the omitted parts are inserted as distributed and concentrated loads at the plate to which they are actually applied. The vibration is more probable in the direction of the two sides where there is no reinforcement stud (in the axial direction of the shafts). Consequently these shafts are not involved in it and can be omitted for greater simplification in the analysis. The first mode of vibration of the structure is shown in Figure 5. The value of the frequency of the structure in this mode, which is the minimum frequency, is 67 Hz and is more than the maximum stimulation's frequency, which is 3000 rpm. Therefore, the resonance would not occur and the design is dynamically safe.

4.2. Planetary gearbox

The planetary gearboxes are chosen from REGGIANA gearboxes. Different parameters are introduced by the producer:

- input speed;
- gearbox ratio;
- output torque;
- correction factor;
- necessary life.

The parameters introduced above should be specified to choose a specific gearbox of this type. The working conditions during the tests are variable, because the torques and speed are variable. The following formulas are offered by the producer for calculating the equal speed and torque in such cases.

$$T_{2r,eq} =$$

$$\sqrt[6.7]{\frac{T_{2r,1}{}^{6.7} \cdot n_{2r,1} \cdot t_1\% + T_{2r,2}{}^{6.7} \cdot n_{2r,2} \cdot t_2\% + \dots + T_{2r,i}{}^{6.7} \cdot n_{2r,i} \cdot t_i\%}{n_{2r,1} \cdot t_1\% + n_{2r,2} \cdot t_2\% + \dots + n_{2r,i} \cdot t_i\%}};$$

(1)

$$n_{2r,eq} = \frac{n_{2r,1} \cdot t_1\% + n_{2r,2} \cdot t_2\% + \dots + n_{2r,i} \cdot t_i\%}{100\%},$$

(2)

$T_{2r,\,eq}$ here is the equivalent output torque needed, t_i, s – the time periods of the presence of each torque, and $n_{2r,\,eq}$ – the needed output speed. $T_{2r,\,i}$ s and $n_{2r,\,i}$ s also account for the different torques and speeds respectively.

Based on Equation (3), in which P, T and ω account for power, torque, and speed, respectively, it is clear that

the maximum torque occurs with the maximum power and minimum speed.

$$P = T \cdot \omega.$$

(3)

The values of the input torque and speed are considered to be 94 kN·m and 2400 rpm based on the common tests for high power gearboxes. For lower planetary gearbox's ratios, lower input torques are needed to induce a specified torque in the system. The minimum ratio among the available choices is 3.4.

Based on the gearbox's catalogue (Reggiana Riduttori S.R.L. 2016) and the operating condition of the gearbox, the correction factor is set to be 0.7. So, the corrected equal torque is 0.658 kN·m.

Due to the information in the gearboxes' catalogues (Reggiana Riduttori S.R.L. 2016), the corrected output torque equals 2237 kN·m; therefore, the usage of gearbox sizes of more than 310 is possible. Due to the corrected equal torque and equal speed, the gearbox's life for minimum ratios 310, 510 and 710 equals 1152,
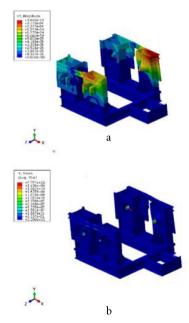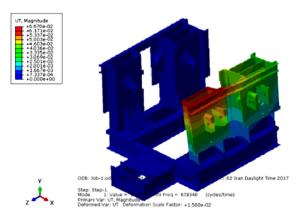

Fig. 4. a) displacements; b) stresses

Fig. 5. The first mode of natural frequencies

2525 and 4730 hours (Reggiana Riduttori S.R.L. 2016). Due to the derived life times, the gearbox with a size of 510 is selected. The maximum input speed for this gearbox is 3500 rpm (Reggiana Riduttori S.R.L. 2016), which is more than the maximum speed in the system (2600 rpm). Heat capacity $\left(P_t\right)$ of this gearbox is 21 kW, and, by considering the correction factor according to the catalogue (Reggiana Riduttori S.R.L. 2016), the heat capacity would be 8.85 kW. Because of the high input
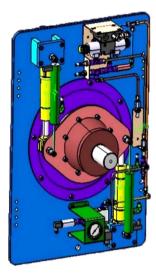

Fig. 6. System of torque generator

Fig. 7. Hydraulic circuit of the torque generator system

power (300 kW), an external cooling system should be considered for its lubricating oil.

For rotating the aforesaid gearbox around its axis, two planes are attached to it at two sides (Fig. 6).

The first one is the plane for rotation and the second one is the arm for inserting torque. The pin which connects these two planes is connected to the hydraulic actuator, so the force is transferred to the planetary gearbox by these two planes. The rotation in the ring of the planetary gearbox is caused by linear hydraulic actuators. The traveling course of the hydraulic jacks is 60 mm, and the coupled forces are inserted at a distance of 175 mm by these jacks, allowing the ring to rotate to up to 20 degrees. The torque required for rotating the ring equals the difference between the planetary gearbox's input and output torque. Therefore, considering that the torque generator system is placed at the output of the test gearbox, the required torque is obtained from Equation (4), in which T and T_i account for the output and input torque, and η and R are the planetary gearbox's efficiency and ratio, respectively:

$$T =(\eta R -1)T_{in}. \qquad (4)$$

Based on (3), the torque required for rotating the ring equals 3.5 kN·m. Considering that the maximum torque is applied when the arm and the jacks are perpendicular to each other, the jacks should endure a maximum force of 1000 N. Figure 4 shows the maximum stress and displacements in the two arms which transfer the torque under two 1000 N loads. As seen, the maximum stress occurs in the two holes, and its magnitude is 3.2 MPa. Considering the material to be structural steel with a yield stress equal to 200 Mpa, the safety factor would be 6. The diameter of the pins which are linked to the ends of the jacks is 20 mm. There are also some displacement sensors that are attached to these pins. The magnitude of the rotation of the ring is measured from the elongation of the pins due to the shear caused by the jacks' loading. The shear stress in the pins caused by applying a 1000 N load is 16 MPa, so steel can be used.

4.3. Hydraulic circuit

The hydraulic circuit designed for controlling the movement of the actuators is shown in Figure 7.

The inner diameter of the cylinders is 40 mm, and the 10 kN force on them causes a pressure of 8 MPa. The driving force of the system is produced by a hydraulic power pack which has a three phase electrical motor, a positive displacement pump with constant flow, a container, a safety valve, and a pressure indicator. The maximum pressure of the torque generator system is 80 bar, so the power pack with the maximum condition pressure of 140 bar is selected and is able to produce a 0.8 lit/min flow in 1500 rpm. The power needed for rotating this pump is derived from the following equation:

$$P = \frac{pQ}{60\eta}. \tag{5}$$

Here P, p, Q, and η, account for power, pressure, flow rate, and efficiency of the pump, respectively. According to Equation (5) and considering the efficiency to be 85% with a pressure of 140 bar and a flow of 0.8 lit/min, the power needed for rotating the pump equals 0.22 kw and the required toque is 1.3 N·m, the power of the power pack's electrical motor is 0.4 kw, whereas the container's capacity is 9 litters. During the tests, the power pack is on continuously, so for prevention of a sudden increase in the power pack's pressure, a safety valve is used. For more safety, a pressure sensor in the circuit used for controlling the system's torque can also be used for monitoring the pressure and sending commands to the control valve to evacuate the pressure. To shift the direction of the hydraulic actuators, a 4/3 directional control valve is used. The neutral condition of the valve is chosen, so that the output of the pump is linked to the container, and thus the pump would be in a no-load condition during operation. The maximum pressure of the directional valve is 350 bar, and the maximum flow is 100 lit/min.

In addition, a flow control valve is used to set and control the speed of the displacement of the actuators. The maximum pressure of this valve is 140 bar and its maximum flow is 11 lit/min. The procedure of controlling the speed is done by limiting the injected flow during the forward movement of the cylinders as well as limiting the flow vacuuming during their backward movement. In case of power outage, an emergency evacuation line is considered for the elimination of the actuator's pressure and dynamic load. For the purpose described above, a 2/2 poppet valve, which has less leakage than other valves, is used in the line. This emergency line could also be used in situations where a fast return of the actuator is necessary. Also, a one direction valve is used to pass the flow to the back of the actuators in the aforesaid situations in order to prevent vacuity.

4.4. Control system design

Torque control

For controlling the torque applied by the actuator system and also keeping it stable during the change of the speeds in the system, a PID controller is used. A diagram of this controller is shown in Figure 8.

In this diagram, the torque changes because of the rate of motor speed change. This torque is considered as a disturbance in the controlling loop; therefore, the other sources of disturbance are ignored because of their relatively low effect.

Considering that the maximum operating pressure of the torque generator system is 80 bar, also the maximum fluid flow needed in the system as well as the available proportional valves, a servo valve among the MOOG G761 3004 series is used. The first and second order transform function of these valves is derivable due to their structure and is provided by the producer (Thayer 1965). The second order equation is shown in Eq. (6):

$$\frac{Q}{i}(s) = \frac{k_{sv}}{1 + 2\zeta\left(\dfrac{s}{\omega_n}\right) + \left(\dfrac{s}{\omega_n}\right)^2}. \tag{6}$$

Here i, k_{sv}, ζ and ω_n indicate the electricity current sent from the controller, flow factor of the valve, damping ratio of the valve's spring, and natural frequency. The values of parameters k, ω_n and ζ are given in Table 1.

Table 1. Specifications of the system (Li, Thurner 2013)

System	k_{sv}	ω_{sv}	ζ	ω_n
MOOG G761-3003	0.0114	160	0.9766	343
MOOG G761-3004	0.0230	160	1.0012	343

$$\frac{q}{i}(s) = \frac{k_{sv}}{1 - \zeta^2 + \zeta^2 + 2\zeta\left(\dfrac{s}{\omega_n}\right) + \left(\dfrac{s}{\omega_n}\right)^2} =$$

$$\frac{\left(k_{sv} \cdot \omega_n \middle/ \sqrt{1-\zeta^2}\right) \cdot \left(\sqrt{1-\zeta^2}\right) \cdot \omega_n}{\left(1-\zeta^2\right) \cdot \omega_n{}^2 + \left(\left(s\right) - \left(-\zeta \cdot \omega_n\right)\right)^2}; \tag{7}$$

$$\frac{Q}{I}(t) = \left(k_{sv} \cdot \omega_n \middle/ \left(\sqrt{1-\zeta^2}\right)\right) \cdot e^{-\zeta\omega_n t} \cdot \sin\left(\left(\sqrt{1-\zeta^2}\right)\omega_n t\right). \tag{8}$$
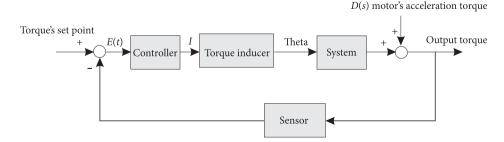

Fig. 8. Loop of the torque generator system's control

The equations of the cylinder system are as follows:

$$\Delta T_{torquer} = \Delta\theta \cdot k_{eq};　\qquad (9)$$

$$\Delta\theta = \Delta\theta_0 (n-1);　\qquad (10)$$

$$\Delta\theta_0 = \frac{2\Delta x}{D};　\qquad (11)$$

$$\Delta x = \frac{V}{A};　\qquad (12)$$

$$\Delta T_{torquer} = \frac{2V(n-1)\cdot k_{eq}}{A\cdot D}.　\qquad (13)$$

In Equations (7) to (13), A, D, k_{eq}, θ and V are the Pistons' area, torquer's diameter, equivalent stiffness of the whole system, and volume of the displaced liquid in cylinders, respectively. The magnitude of the torque the system should apply equals the torque induced in the system based on the rate of the motor speed change. An important case which should be taken into account is the course of the cylinders and its limit. This range causes an upper limit in the torque induced, which is computable. In this system, the input of the valves is the current, and the output is the torque. We have a set point for each test which is equal to the constant torque needed to be applied to the system in each moment of the test. For deriving the transform equation of the present system, as the relation between the volume of the flow and the torque is known (Eq. (13)), deriving the relation between the fluid volume and the current is the key. The related equations are provided below:

a

b

c

Fig. 9. Responses: a) response of the system to a pulse signal; b) response of the system to a step signal; c) response of the system to a sine signal

$$V = \int Q\,dt;　\qquad (14)$$

$$\Delta T_{torquer} = \frac{2\left(\int i\left(\frac{k_{sv}\omega_n}{\sqrt{1-\zeta^2}}\right)\cdot e^{-\zeta\omega_n t}\cdot \sin\left(\left(\sqrt{1-\zeta^2}\right)\cdot\omega_n t\right)dt\right)\cdot(n-1)k_{eq}}{A\cdot D} = 2i\left(\frac{k_{sv}\cdot\omega_n}{\sqrt{1-\zeta^2}}\right)\cdot$$

$$\left(\frac{e^{-\zeta\omega_n t}\left(-\zeta\omega_n\cdot\sin\left(\left(\sqrt{1-\zeta^2}\right)\cdot\omega_n\cdot t\right)-\left(\sqrt{1-\zeta^2}\right)\cdot\omega_n\cdot\cos\left(\left(\sqrt{1-\zeta^2}\right)\cdot\omega_n\cdot t\right)\right)}{\left(\zeta\omega_n\right)^2+\left(1-\zeta^2\right)\cdot\omega_n^2}\right)\cdot\left(\frac{(n-1)\cdot k_{eq}}{A\cdot D}\right). \qquad (15)$$

So the transform function would be:

$$\frac{T}{i} = \frac{2k_{sv}\cdot\omega_n\cdot e^{-\zeta\omega_n t}\left(-\zeta\omega_n\sin\left(\left(\sqrt{1-\zeta^2}\right)\cdot\omega_n\cdot t\right)-\left(\sqrt{1-\zeta^2}\right)\cdot\omega_n\cdot\cos\left(\left(\sqrt{1-\zeta^2}\right)\cdot\omega_n\cdot t\right)\right)\cdot(n-1)\cdot k_{eq}}{\left(\sqrt{1-\zeta^2}\right)\cdot\left(\left(\zeta\omega_n\right)^2+\left(1-\zeta^2\right)\cdot\omega_n^2\right)\cdot A\cdot D}. \qquad (16)$$

A control model is made in MATLAB according to the equation presented above, and the responses of the designed system to various inputs are shown in Figures 9a–c.

Controlling the other parameters

A PLC is used for controlling the other parameters such as pressure, temperature, motor speed, motor, and other component vibration in the system. The pressure in the following parts is controlled:

– hydraulic system oil;
– gearbox oil;
– torque generator oil;
– input water of the cooler.

The actions for controlling the temperature and pressure are similar and contain two steps – sending the

alarm and turning the system off. The input and output temperature of the gearbox oil and the input and output water temperature of the cooling tower are also controlled. There are some pumps (due to the torque inducing system) in the torque generator gearbox oil circuit, so the temperature oil of these pumps should also be controlled. This circuit is shown in Figure 10.

The motor's controller is in the drive, and the commands for changing the speed are transferred from the console to the PLC by a pulse generator, and from the PLC to the drive by a PROFIBUS network. Vibration digital sensors are mounted on the rotary components and are connected to the PLC's input with 24 voltage. In cases when the vibration amplitude goes beyond the limit, the testing procedure would be stopped.
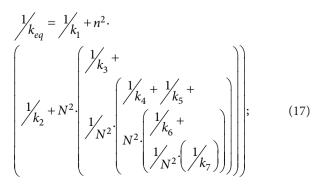
5. Modelling of the system

To ensure the operation of the system, a mechanical model was created in AMESIM, and the response of the system to different inputs has been investigated. In this model, the torque inducing system, including the actuators and cylinders as well as the hydraulic circuit has been modelled and simplified by an angle generator element. The shafts are modelled as an angular spring with angular stiffness equal to the same parameter in the shafts, the rotary inertias are also considered. The values of all parameters are equal to the ones in the actual system. This model is shown in Figure 11a. The system can also be simplified by an equivalent stiffness and equivalent inertia to an open-loop system, as shown in Figure 11b.

5.1. Analysing the response of the system's model

The input of the system (angle of rotation) is inserted as a ramp function with a delay. The torque induced at the two ends of the equivalent open-loop system is shown in Figure 12.

5.2. Equivalent parameters of the system

As indicated in 5–1, the system could be simplified by determining its important mechanical equivalent parameters so that analysing it and deriving the equations of the state would become easier. The considered parameters are equal stiffness and equal rotary inertia, and, due to the law of the conservation of energy, these parameters are calculated using Equations (17) and (18).

$$
\frac{1}{k_{eq}} = \frac{1}{k_1} + n^2 \cdot \left(\frac{1}{k_2} + N^2 \cdot \left(\frac{1}{k_3} + \frac{1}{N^2} \cdot \left(\frac{1}{k_4} + \frac{1}{k_5} + N^2 \cdot \left(\frac{1}{k_6} + \frac{1}{N^2} \cdot \left(\frac{1}{k_7} \right) \right) \right) \right) \right); \tag{17}
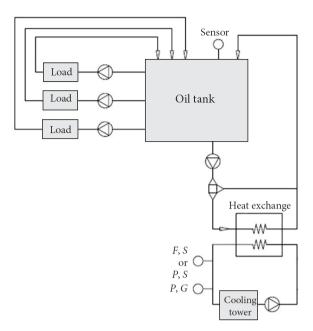$$

Fig. 10. Circuit of the oil cooling system of the torque generator gearbox
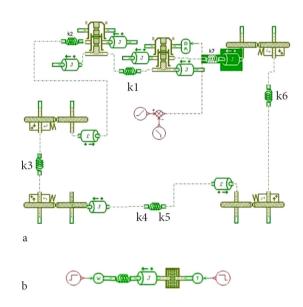

Fig. 11. Modelling results: a) simulated model of the system in AMESIM; b) simplified open-loop model of the system in AMESIM
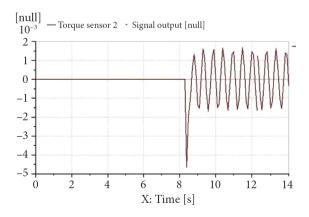

Fig. 12. Torque generated in the model of the system due to a ramp torsion input

$$J_{eq} = 2J_s + J_1 + \left(\frac{1}{n}\right)^2.$$

$$\left(J_P + J_{g1}\right.$$
$$+J_2 + \left(\frac{1}{N}\right)^2 \cdot \left(\begin{array}{l} 2J_{g2} + J_3 \\ +2.J_{g1} + J_4 \\ +N^2 \cdot \left(+\left(\frac{1}{N}\right)^2 \left(\begin{array}{l} J_{g2} + J_3 + J_2 \\ +N^2\left(J_{g1} + J_2 + J_{PC}\right) \end{array}\right)\right) \end{array}\right).$$

$$\tag{18}$$

The parameter X_i is related to the *i*th element.

Placing the values of the parameters into Equations (19) and (20), we obtained the equivalent parameters:

$$k_{eq} = 6231.709 \ \frac{\text{N}}{\text{m}}; \tag{19}$$

$$J_{eq} = 0.5265 \ \text{kg·m}^2. \tag{20}$$

By using these equivalent parameters, the open-loop model is completed. The responses of this model and the main model are compared. The equality of these two sets of responses reveals the validity of the simplified model and the mathematical model used to derive the equivalent parameters. Also, based on the results shown in 5–1,
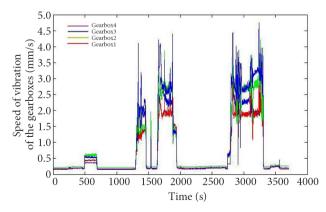

Fig. 13. Test rig

Fig. 14. Vibrations of the gearboxes during the test versus time

the absolute value of the torque at $t = 16$ s according to the software data is about 0.343566×10^{-3}, and the sum of the rotations along the rotational elements in the model equals 55.133×10^{-9}. According to these values, from Eq. (10), the equivalent rotational stiffness equals 6231.585, which is nearly the same as the equivalent stiffness calculated by Eq. (6):

$$T = k \cdot \left(\sum \theta\right). \tag{21}$$

Also, according to the natural frequency of the system (due to the application of a constant torque to the system of inertia and spring), using Eq. (22), the equivalent inertia equals 0.53 kg·m² approximately. These results also show the validity of the formulas in this case:

$$\omega_n = \sqrt{\frac{k_{eq}}{J_{eq}}}. \tag{22}$$

6. Conclusions and results

The mechanical closed-loop gearbox test rig is capable of testing orthogonal gearboxes in various conditions, including different torques and speeds, with high accuracy. It can be used for fault detection of high power gearboxes with high economic and energy efficiency. The designed rig is also dynamically and statically safe and its design validity has been investigated. The results of the simulation of the torque inducer system in MATLAB reveal that the system's responses are steady and reach their goal within 5 seconds. The results of the system simulation in AMESIM and investigation of the system's responses reveal that the whole system is steady, and that the equivalent parameters as well as the simplified open-loop model are valid. The energy consumption of the system is computable, and by computing the energy losses along the loop, the testing of up to four orthogonal gearboxes using the present rig is also possible. The final product of the research is presented in Figure 13.

The whole system has been tested with different torques and speeds, and the resulting vibrations of the gearboxes are shown in Figure 14. The loses of energy in the system under different conditions are shown in Figures 15a–b.

As shown in Figure 14, the maximum speed of vibration in the gearboxes is 4.5 mm/s, which is acceptable. This result also shows the validity of the vibration simulations in the system. According to Figure 15, the losses in the system decrease with increasing test power; the maximum testing power reaches about 11% of the whole power used. This means that the closed-loop system is best for high power testing and that in this specific case efficiency can reach 89%. These figures also show that the system has a base loss dependent on speed. Consequently, the efficiency is much better in high speeds.
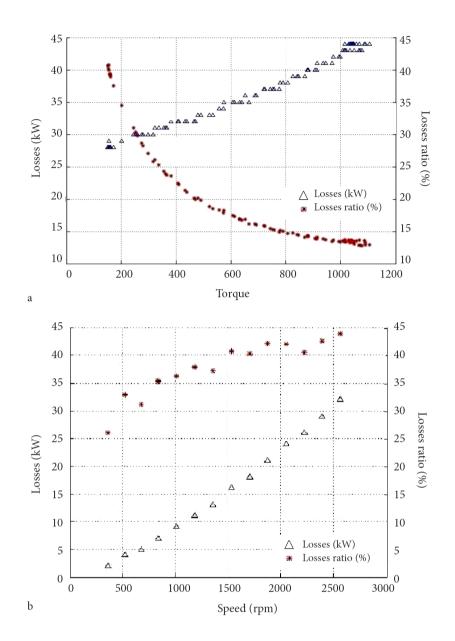
Fig. 15. a) Losses and loss ratio of the system with constant 3000 rpm speed and variable torque; b) losses and loss ratio of the system with constant 150 N.m torque and variable speed

Notations

η	Efficiency	J_{pc}	Sum of the planet's and ring's rotary inertia
θ	Rotation	J_s	Sun's rotary inertia in planetary gearbox
$\Delta\theta$	Total rotation in the whole model	J_{eq}	Equivalent rotary inertia
$\Delta\theta_0$	Rotation in the planetary gearbox's ring	k_{eq}	Equivalent stiffness
ζ	Damping factor	k_{sv}	Flow Factor
ω	Rotary speed	n	Planetary gearbox's ratio
ω_n	Natural frequency	N	Orthogonal gearbox's ratio
A	Piston's area	$n_{2r,eq}$	Equivalent output speed needed
D	Vertical distance between two cylinders	p	Operating pressure
i	Current	P	Power
J_{g1}	Pinion's rotary inertia in orthogonal gearbox	Q	Volumetric Flow Rate
J_{g2}	Gear's rotary inertia in orthogonal gearbox	R	Gearbox's ratio
J_i	Rotary inertia of the components of k_i	t	Time
J_p	Planet's rotary inertia in planetary gearbox	T	Torque
		t_i	i'th time period

T_{in} Gearbox's input torque
ΔT Torque difference
$T_{2r,eq}$ Equivalent output torque needed
V Volume
ΔX Displacement

References

Arun, A. P., *et al.* 2014. Gear test rig – a review, *International Journal of Mechanical & Mechatronics Engineering* 14(5): 16–26.

de Gevigney, D., *et al.* 2012. Thermal modelling of a back-to-back test machine: application to the FZG test rig, *Journal of Engineering Tribology* 226(6): 501–515. https://doi.org/10.1177/1350650111433243

Fernandes, C. M. C. G., *et al.* 2014. Torque loss of type C40 FZG gears lubricated with wind turbine gear oils, *Tribology International* 70: 83–93. https://doi.org/10.1016/j.triboint.2013.10.003

Fernandes, C. M. C. G., *et al.* 2015a. Gearbox power loss. Part II: friction losses in gears, *Tribology International* 88: 309–316. https://doi.org/10.1016/j.triboint.2014.12.004

Fernandes, C. M. C. G., *et al.* 2015b. Gearbox power loss. Part III: application to a parallel axis and a planetary gearbox, *Tribology International* 88: 317–326. https://doi.org/10.1016/j.triboint.2015.03.029

Fernandes, C. M. C. G., *et al.* 2016. Energy efficiency tests in a full scale wind turbine gearbox, *Tribology International* 101: 375–382. https://doi.org/10.1016/j.triboint.2016.05.001

Hollingworth, N. 1987. A four-square chain wear rig, *Tribology International* 20(1): 3–9. https://doi.org/10.1016/0301-679X(87)90002-8

Handschuh, R. F.; Rohn, D. A. 1989. Efficiency of a helicopter transmission planetary reduction stage, in *5th International Power Transmission and Gearing Conference*, 25–28 April, Chicago, United States.

Khodwe, S. S.; Prabhune, S. S. 2015. Design and analysis of gearbox test bench to test shift performance and leakage, *International Journal of Advance Research and Innovative Ideas in Education* 1(2): 270–280.

Li, L.; Thurner, T. 2013. Accurate modelling and identification of servo-hydraulic cylinder systems in multi-axial test applications, *Ventil* 19(6): 462–470. http://www.revija-ventil.si/data/strokovni-clanki/19-2013-6/li_graz.pdf

Manoj, V., *et al.* 2003. Development of a power re-circulating gear test rig, in *11th National Conference on Machines and Mechanisms,* 18–19 December, New Delhi, India.

Miláček, O. 2004. *Endurance testing of automotive gearbox*: Master thesis. Prague, University of Prague.

Markowski, T., *et al.* 2010. Numerical model of aviation gearbox test rig in a closed loop configuration, *Aviation* 14(1): 3–11. https://doi.org/10.3846/aviation.2010.01

Maia, A., *et al.* 2014. A method for evaluating the dynamic behavior of a gear test rig, in *23rd SAE Brazil International Congress and Display*, 30 September–2 October, São Paulo, Brazil.

Reggiana Riduttori, S. R. L. 2016. *Planetary gearboxes' catalogue, product catalogue* [online], [cited 09 December 2017]. Available from Internet: http://www.hydront.ru/files/Standart_gear_drives_ENG.pdf

Thayer, W. J. 1965. MOOG Inc. controls division, *Transfer introduction functions for Moog Servo valves* [online], [cited 09 December 2017]. Available from Internet: http://www.servovalve.com/technical/new_tb_103.pdf

Yin, M., *et al.* 2016. Theoretical and experimental studies on dynamics of double-helical gear system supported by journal bearings, *Advances in Mechanical Engineering* 8(5): 1–13. https://doi.org/10.1177/1687814016646977